Indian Geotech J (June 2018) 48(2):316–326
https://doi.org/10.1007/s40098-017-0280-4

ORIGINAL PAPER

Effect of Geocomposite Layers on Slope Stability Under Rainfall Condition

Dipankana Bhattacherjee[1] · **B. V. S. Viswanadham**[1]

Received: 9 May 2017 / Accepted: 27 September 2017 / Published online: 12 October 2017

Abstract Slope instability and associated loss of matric suction under rainfall condition is a serious global issue, and deserves special attention. The objective of the present paper is to investigate the effect of inclusion of a special variety of geosynthetic material, referred to as geocomposite (or dual-function hybrid geosynthetic) within slopes subjected to rainfall. In this regard, centrifuge based physical modelling was performed on a model silty-sand slope having 7.2 m height (prototype scale) and 2V:1H inclination at 30 gravities using the 4.5 m radius centrifuge facility available at IIT Bombay, India. A rainfall simulating assembly was designed and developed for the above study, capable of producing fine mist at a uniform rate during in-flight testing using specially designed pneumatic nozzles (intensity range: 2 mm/h to as high as 80 mm/h). The surface settlements, displacement profile, strain experienced by reinforcement layers, and pore water pressure profiles developed during rainfall were investigated in the unreinforced and reinforced slope models. It was observed that, the unreinforced slope model experienced excessive settlement and increasing phreatic levels with rainfall, leading to catastrophic failure. On the contrary, the geocomposite reinforced slope was stable under rainfall condition, and experienced negligible deformation with progress of rainfall, the maximum peak strain value being as low as 8.01%. Further, the inclusion of geocomposite layers provided preferential drainage channels within the slope, and resulted in reduction of pore water pressure values by almost 47%, thereby indicating the importance of coupling the functions of reinforcement and drainage simultaneously within low-permeability slopes subjected to rainfall. The above finding facilitates the use of locally available low-permeable soils in construction of reinforced soil walls/slopes, thereby economizing the project. Further, use of marginal soils in combination with geocomposites (or hybrid geosynthetics) can prevent the unsustainable mining of natural sand deposits for construction purposes, while catering to the problem of scarcity of good quality permeable granular materials in recent times.

Keywords Geocomposites · Rainfall · Low-permeable soil · Slope stability · Centrifuge model test · Image analysis

Introduction

Recently, the frequency of rainfall-triggered landslides has been increasing globally, coincident with the effects of climate change, leading to thousands of deaths and severe damages to infrastructures. In field case histories, numerous instances are cited where failure occurred in natural or excavated soil slopes simply due to rainwater infiltrating in an otherwise stable slope. In the last decade, several cases of rainfall-induced disasters have been reported in India (number exceed 2700 annually, as per the *Geological Survey of India*), a few of which include the major landslide blocking tracks along a section of the Konkan railway (2010), the cloudburst conditions in Uttarakhand rendering masses homeless (2013, 2014 and 2016), and the landslides along the Mumbai–Pune expressway (2015) and Arunachal

✉ Dipankana Bhattacherjee
dipankanabhattacherjee@iitb.ac.in;
dipankanabhattacherjee@gmail.com

B. V. S. Viswanadham
viswam@civil.iitb.ac.in

[1] Department of Civil Engineering, Indian Institute of Technology Bombay, Powai, Mumbai 400076, India

Pradesh (2016), all of which were triggered by heavy monsoon rain. As per the archive on *Global Weather and Climate Extremes* compiled by World Meteorological Organization (WMO), the highest average annual total precipitation till date observed over a span of 10 years is 11,872 mm (467.4 inch) recorded in Mawsynram, Meghalaya, India. Further, the annual statistical review report of the *Centre for Research on the Epidemiology of Disasters* [1] reveals that, in the year 2016, almost 75% of the natural disasters that occurred in the country may be attributed to rainfall, and the estimated average losses due to rainfall-triggered landslides (especially in the Himalayan regions) exceed Rs. 550 crores/year [2]. The primary reason behind the instability may be attributed to the scarcity of good quality granular material (having high co-efficient of permeability) in recent times, arising out of rapid and unsustainable mining of natural sand deposits over the years. Basu et al. [3] reported that the construction industry accounts for about 40% of the global energy consumption and depletes substantial quantity of sand and gravel in the process. Such depletion of natural resources in course of construction of geotechnical projects interfere with the over-all environmental and ecological balance, affecting the society at large. As for example, sand over-mining leads to disturbances in aquatic ecosystem, and produces disastrous impacts on rivers, including uncontrolled erosion, sliding failure along the river banks, degradation of river bed, undermining of bridge supports and eventual deterioration of river water quality. This necessitates sustainable planning in infrastructural projects by incorporation of alternative construction materials capable of catering to the technical requisites of permeable granular soil, while being available locally in substantial quantity. In the field, during construction of reinforced soil walls/slopes, absence of good quality permeable sand leads to the eventual use of low-permeability soils (termed as marginal soils) available locally at the construction site [4]. This leads to pore water pressure build-up under the impact of rainfall due to the inefficiency of the marginal soil to dissipate the excess water generated within the slope during the rainfall event, in addition to excessive deformation and reduction in shear strength at the interface of soil and reinforcement [5, 6].

The objective of the present study is to examine an alternative solution of reducing pore water pressures and deformations in low-permeable soil slopes subjected to rainfall by inclusion of a special variety of geosynthetic material, viz. geocomposites or dual-function hybrid geosynthetic within the slope. This can lead to significant reduction in project costs and prevent the depletion of natural resources (in this case riverine sand deposits), thereby maintaining a sustainable ecological balance in geotechnical construction. Geocomposite is an assembled material possessing both in-plane drainage and reinforcement characteristics derived from a nonwoven geotextile and geogrid respectively [7–11]. The basic philosophy behind the production of geocomposite materials is to combine the best features of different materials in such a way that specific applications are addressed in the optimal manner and at minimum cost. In the literature, the use of permeable inclusions as an effective alternative to dissipate the pore pressure build-up in reinforced low-permeable slopes have been suggested [12–14]. The importance of reinforcement function in maintaining stability of an unsaturated embankment was reported by Iryo and Rowe [15]. However, till date, studies on the potential coupling of reinforcement and drainage functions in the form of geocomposite layers are limited, especially with respect to investigation of slope stability under rainfall condition in a geotechnical centrifuge. Hence, this forms a topic of major research interest.

Materials and Methodology Involved

Model Materials and Scale Factors

The model soil used in the present study was formulated by blending locally available fine sand and commercially available kaolin in the ratio of 4:1 by dry weight, in order to represent the geotechnical properties of locally available soil with low permeability found in major portions of India. The model geocomposite material (refer Fig. 1) was developed by combing the functions of drainage provided by permeable non-woven geotextile (N1) with reinforcement of woven geogrid (G1) in an integral manner, so as to depict the characteristics of commercially available existing prototype hybrid geosynthetic materials. The relevant properties of model soil and geocomposite material are summarized in Tables 1 and 2 respectively. In order to replicate similar stress history and retain identical state of stresses in model soil as that existing in-field, centrifuge based physical modelling technique was adopted, where the body forces of model geomaterials are increased by applying centrifugal acceleration of high gravities (Ng) relative to that of earth's normal gravity (g). The modelling of geogrid component of hybrid geosynthetic in centrifuge was done based on the scaling considerations proposed by Viswanadham and König [16], Viswanadham and Jessberger [17] and Rajesh and Viswanadham [18], whereas, the parent geotextile component was scaled based on identical transmissivity requirements between model and prototype, as outlined in Raisinghani and Viswanadham [19].

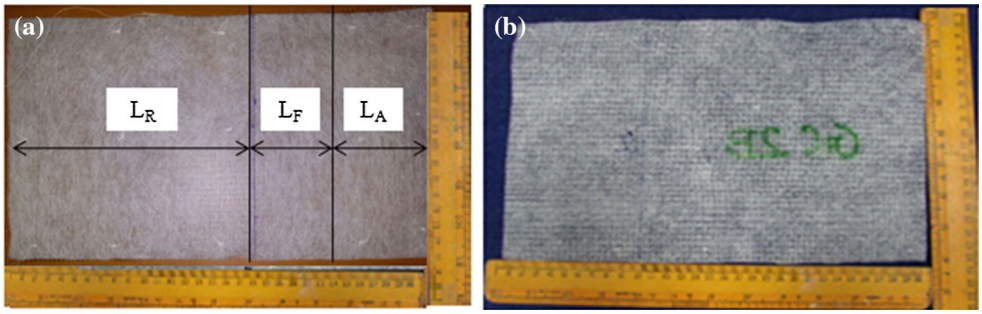

Fig. 1 Model geocomposite material used in reinforced slope. **a** Front: non-woven geotextile component, **b** back: woven geogrid component

Table 1 Properties of model soil used in present study

Quantity	Value
Specific gravity, G_s	2.62
Particle size distribution	
Sand [0.075–4.75 mm] (%)	80
Silt [0.075–0.002 mm] (%)	10
Clay [< 0.002 mm] (%)	10
Atterberg limits	
Liquid limit (%)	_[b]
Plastic limit (%)	NP[a]
Plasticity index (%)	_[b]
Soil classification (USCS)	SM
Compaction characteristics[c]	
Maximum dry unit weight, γ_{dmax} (kN/m^3)	18.75
Optimum moisture content (%)	9
Permeability[d]	
Coefficient of permeability, k (m/s)	1.54×10^{-6}
Shear strength parameters[e]	
Cohesion, c′ (kPa)	12
Angle of internal friction, ϕ′ (°)	28

[a]NP, Non Plastic

[b]Not relevant

[c]Standard proctor

[d]Falling head tests performed on moist-compacted soil at γ_{dmax} and OMC

[e]CU Triaxial tests (drained) conducted on moist-compacted soil at γ_{dmax} and OMC

Rainfall Simulating Assembly

A robust rainfall simulating system was designed and developed for inducing rainfall at high gravities, by taking into account the relevant scaling laws related to modelling of rainfall in centrifuge, as outlined in Dell'Avanzi et al. [20], Tamate et al. [21] and Bhattacherjee and Viswanadham [22], presented in Table 3. Detailed description of design philosophy and various components of the developed rainfall simulator are outlined in Bhattacherjee and Viswanadham [22]. The simulator is capable of producing rainfall in the form of fine mist at high gravities using specially designed pneumatic nozzles. The lower and upper limits of rainfall intensities that can be replicated with the developed set-up vary from as low as 2–80 mm/h, which is the maximum recorded intensity till date globally in real-life full-scale structures. An additional advantage includes the fact that the intensity and duration of rainfall can be regulated at any point of time in-flight condition to replicate all varieties of real-life natural hazards, ranging from long-term medium intensity rainfall (similar to monsoon showers and antecedent rainfall patterns) to a short spell of

Table 2 Properties of model geocomposite materials

Property	Geosynthetic type		
	Geogrid	Geotextile	Geocomposite
Composition and type	Woven (G1)	Non-woven polypropylene (N1)	G1N1
Area weight (g/m^2)	11.4	46	59.4
Thickness, t_g at 2 kPa (mm)	–[a]	0.66	0.91
Percentage open area, f (%)	97.43	–[a]	–[a]
Ultimate Tensile load, T_{ult} (kN/m)[b]			
Machine direction	0.796	0.23	1.12
Cross-machine direction	0.664	0.11	0.78
Ulitimate strain, ε_{ult} (%)[b]			
Machine direction	25	5.77	31.21
Cross-machine direction	27.25	48.14	78.46
Transmissivity, θ_g ($\times$ 10^{-6} m^2/s)[c]	–[a]	0.38	1.72
In-plane permeability, k_g ($\times$ 10^{-3} m/s)	–[a]	0.57	1.89
Bond skin friction, τ_b (kPa)[d]	10.47	–[a]	12.49

[a]Not relevant/carried out

[b]Wide-width tensile tests as per ASTM D 4595 (2005)

[c]Radial transmissivity as per ASTM D 6574 (2006) reported at normal stress of 20 kPa, and defined as $\theta_g = k_g\, t_g$, where k_g is the in-plane permeability of geosynthetic (m/s)

[d]Modified direct shear test

Table 3 Scale factors for modelling rainfall at high gravities

Parameter	Unit	Prototype	Ng Model
Amount of rainfall	mm	1	1/N
Duration of rainfall (t)	h	1	1/N^2
Precipitation intensity (r)[a]	mm/h	1	N
Terminal velocity of raindrops (U)	m/s	1	1/N
Impact pressure on ground (P)	Pa	1	1
Soil Suction (ψ)	kPa	1	1

N: Gravity level/Scale factor

[a]For example, $\frac{r_m}{r_p} = N$; m = model; p = prototype

very high intensity rainfall (similar to cloudburst condition). Further, while designing the components of the simulator, special measures were adopted to nullify Coriolis effects on droplet trajectory at high gravities, details of which are outlined in Bhattacherjee and Viswanadham [22].

Centrifuge Testing Procedure and Instrumentation

Centrifuge model tests were performed on unreinforced and geocomposite reinforced slopes subjected to a heavy rainfall intensity of 14.4 m/day (20 mm/h) with the developed rainfall simulator triggered in a 4.5 m radius large beam geotechnical centrifuge facility available at Indian Institute of Technology, Bombay, India. Details of the centrifuge equipment and associated specifications are available in Chandrasekaran [23]. A seepage tank with perforations was placed on the right hand end of the model container (Fig. 2) to maintain an initial ground water table within the soil slopes up to the base prior to rainwater infiltration, and the perforated wall was covered with a thin layer of nonwoven geotextile to prevent clogging of holes by soil particles during rainfall. In addition, a run-off collector was placed on the swing basket of centrifuge to collect the excess water flowing as run-off during tests.

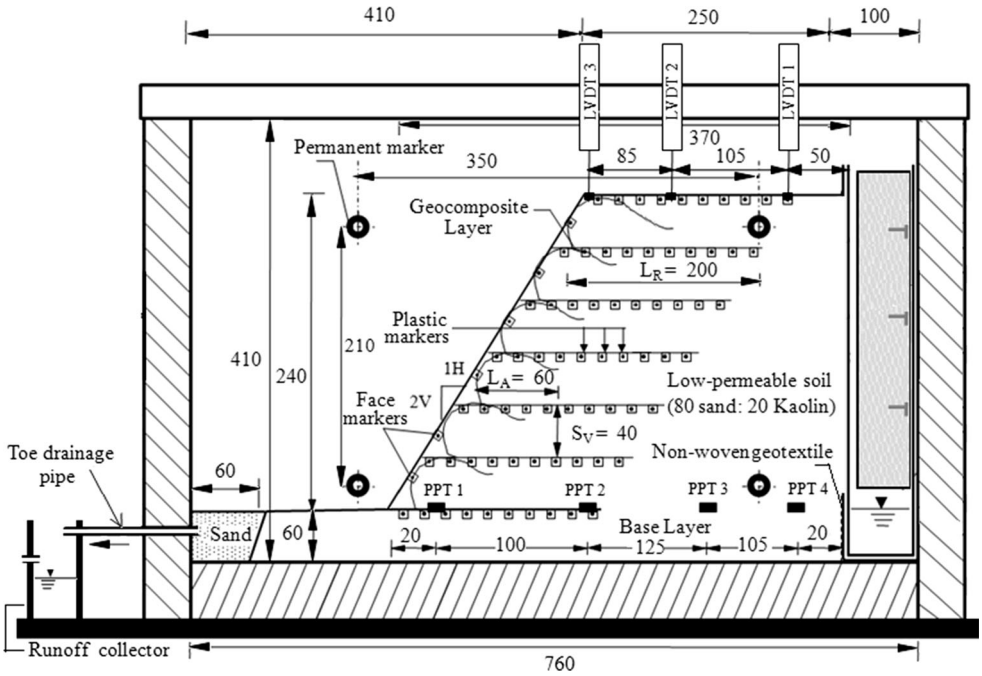

Fig. 2 Details of model test package and instrumentation (all dimensions are in mm)

From here onwards, the dimensions are given in model scale, while those in prototype scale are represented in parenthesis. Centrifuge model tests were carried out at 30 g on a 240 mm (7.2 m) high slope with 60 mm (1.8 m) base layer and a crest width of 250 mm (7.5 m), having an inclination of 63.43° with the horizontal. Selection of 30 g was made due to the fact that, the model unsaturated slope (volumetric water content: 0.3818–0.1826 m^3/m^3 respectively for matric suction between 0.01 and 1000 kPa) was found to have factor of safety just above one numerically at this g level. The model slope, as well as the base layer, was constructed with sand-kaolin mix in the ratio of 4:1 by dry weight, moist compacted at respective γ_{dmax} (18.75 kN/m^3) and OMC (9%). Four pore pressure transducers (PPTs) were placed above the base layer at distances of 20 mm (PPT4), 125 mm (PPT3), 250 mm (PPT2) and 350 mm (PPT1) from the perforated face of the seepage tank, as shown in Fig. 2. Thus, PPT2 was kept at a point vertically below the crest of the slope, PPT3 was at a point vertically below the mid-length of the slope top surface, and PPT1 was placed almost at the toe of the slope. The model was instrumented with three Linearly Variable Differential Transformers (LVDTs) placed at the top of the slope at a distance of 50 mm (L1), 155 mm (L2) and 240 mm (L3) from the edge of the seepage tank for measuring surface settlements induced by rainfall. In addition, L-shaped plastic markers made from thin transparency sheets (20 mm × 10 mm) were embedded within the slope front elevation to track displacements during various stages of the test due to gradual progress of the wetting front. The markers were folded in the middle and white petroleum grease was applied to the side of the marker in contact with the Perspex sheet, to allow for its free movement with soil. The geocomposite material (Fig. 1) was cut to a total length of ($L_A + L_F + L_R$), where L_A is the anchorage length (equivalent to 0.25 times the model slope height, h); L_F is the length along the slope face, and L_R is the length of reinforcement, (taken as 0.85h), and to a width of 200 mm. The topmost layer had an additional wrap-around length equivalent to 0.37h to avoid sloughing failures.

The various stages involved in construction of model soil slopes in centrifuge are presented in Fig. 3a–f. The desired slope inclination was achieved by using a temporary wooden block of same inclination, placed on the right hand side of the container, after compaction of the base layer (Fig. 3a, b). Coloured food dye was placed at the top of each layer after compaction (Fig. 3c, d), in order to trace the movement of infiltrating rainwater as an indicative of phreatic surfaces developed due to progress of wetting front within the soil slope. In addition, a thick bentonite paste was applied along the slope face (Fig. 3e) to arrest movement of soil particles through minute gaps between container wall edges and the slope, and a toe drain made of sand drainage layer (Fig. 2) was provided towards the downstream end of the slope to facilitate free drainage of run-off due to rainfall. After completion of the model (Fig. 3f), the rainfall simulator system consisting of the nozzle hanging assembly, dispenser assembly and water container assembly were mounted on the strong box. A total of eight nozzles were used for conducting tests on model soil slopes, with four nozzles placed above the slope top surface at distances of 50 mm (1.5 m) and 150 mm

Fig. 3 Various stages involved in construction of geocomposite reinforced slope model. **a** Preparation of base layer and placement of PPTs, **b** placement of first geocomposite layer, **c** markers glued on to geocomposite surface to compute strains during test, **d** placement of subsequent layers and markers, **e** wrap-around slope facing, **f** view of completed slope model

(4.5 m) from the crest, while the remaining four nozzles were positioned near the inclined face of the slope with the help of adjustable nozzle hanging rods. The nozzles were suspended at a height of 100 mm (3 m) above the slope top surface, each covering an effective influence area of 100 mm by 100 mm (3 m by 3 m). The results of three centrifuge model tests (T1, T2 and T3) are discussed in the present study, wherein models T1 and T2 are unreinforced with varying water table position and model T3 is reinforced with six layers of geocomposites with an initial water table up to the base of the slope. The duration of centrifuge tests were maintained as 40 min (25 days) from the period of starting rainfall (Model T3), or until failure (Models T1 and T2), whichever occurred first, and the results were analyzed and interpreted in terms of surface settlements, slope displacement profiles, strains experienced by reinforcement layers and pore-water pressure development during rainfall in unreinforced and geocomposite reinforced slopes.

Interpretation of Test Results

Effect of Initial Water Table

The normalized pore water pressures ($u/\gamma h$) values at failure observed for the model slopes T1-T3 are presented in Table 4 for the data corresponding to PPT2 placed at a

Table 4 Summary of centrifuge test results

Parameter	Test Model		
	T1	T2	T3
Time elapsed during rainfall, *t* (days) in prototype dimensions	12.1875[a]	9.375[a]	23.50[b]
$u/\gamma h$[c]	0.427	0.514	0.272
$S_{c,max}/h$	0.375	0.492	0.033
$S_{f,max}/h$	0.096	0.167	0.050
$\varepsilon_{p,max}$	–[d]	–[d]	8.01%

h, height of slope; $u/\gamma h$, normalized pore pressure; $S_{c,max}$, max. crest settlement; $S_{f,max}$, max. deformation along slope face; $\varepsilon_{p,max}$, reinforcement peak strain obtained in reinforced slope model by image analysis

[a]Time corresponding to failure

[b]During penultimate stage of test

[c]For PPT2 placed at distance of 120 mm from the toe of slope

[d]Not relevant

distance of 120 mm (3.75 m) from the toe of the slope, normalized with respect to the unit weight of soil (γ) multiplied by the slope height (h). In order to study the impact of initial water table position on subsequent development of phreatic surfaces during rainfall, models T1 and T2 were subjected to two different conditions of water table, keeping slope dimensions and rainfall intensity constant. In case of model T1, the water table was considered to be located at a significant depth below the slope base, whereas, in model T2, an initial water table was maintained till the base of the slope, similar to test T3, by means of horizontal seepage induced by the seepage tank, as discussed in previous sections. From the summary of centrifuge test results presented in Table 4, it can be observed that the maximum crest settlement at failure for models T1 and T2 were 90 mm (2.7 m) and 118 mm (3.54 m) respectively, which depicts the fact that, due to presence of initial water table, Model T2 is more susceptible to rainfall induced failure and settlements than T1 for the same intensity of rainfall. Similar observations can be made from the high value of normalized pore pressure ($u/\gamma h$) registered by the model T2. Henceforth, to be on the critical side, an initial water table position was considered in the geocomposite reinforced slope model (T3), while studying its stability aspects in a centrifuge under rainfall condition.

Effect of Inclusion of Geocomposite Layers

The variation of normalized pore pressure ($u_{toe}/\gamma h$) with progress of rainfall is presented in Fig. 4, for the data corresponding to PPT 1 placed near the toe of the slope. As evident from Fig. 4 and the values for PPT 2 presented in Table 4, the unreinforced slopes registered high values of $u/\gamma h$ (0.427 for T1and 0.514 for T2: PPT 2) due to rapid loss of matric suction and subsequent build-up of excess positive pore water pressures induced by rainfall, thereby necessitating suitable drainage measures within the slope. Further, the $u/\gamma h$ values reduced by 47% on an average ($u/\gamma h = 0.272$ for T3: PPT 2) with the inclusion of dual-function geocomposites (or hybrid geosynthetic layers) within the slope, thereby highlighting the importance of drainage function (provided by non-woven geotextile component) in maintaining slope stability under rainfall. Figure 5a, b present the variation of surface settlements with horizontal distance from the crest of the slope at various time-intervals during rainfall, till failure/penultimate stage of test, obtained by tracking the top row of plastic markers in conjunction with LVDT data captured in-flight. As evident from Fig. 5a, the surface settlements increased with rainfall in the unreinforced slope model T2 due to gradual propagation of the wetting front, until failure occurred at $t = 15$ min (9.375 days). On the contrary, the geocomposite (G1N1) reinforced slope model T3 experienced almost negligible deformation with progress of rainfall (Fig. 5b), the maximum value being 7.33 mm (0.22 m) at the termination of test at $t = 37.60$ min (23.5 days), thereby indicating the efficacy of geogrid component in providing the necessary reinforcement action under rainfall, and mitigating settlements in low-permeability soil slopes.

The gradual movement of slope face in lateral and vertical direction and strains developed in geocomposite layers with progress of rainfall were investigated for the entire duration of centrifuge tests with the help of Digital Image Analysis (DIA) technique [24]. Images were captured in-flight with a 3.2 Mega Pixel digital camera operating at an interval of 30 s, and digitization was done with

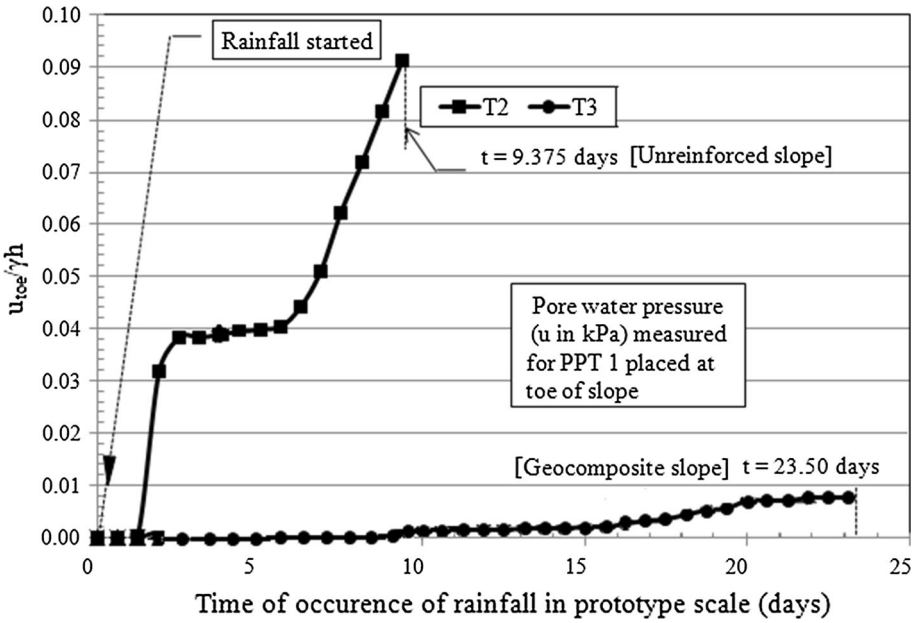

Fig. 4 Variation of pore water pressure with rainfall

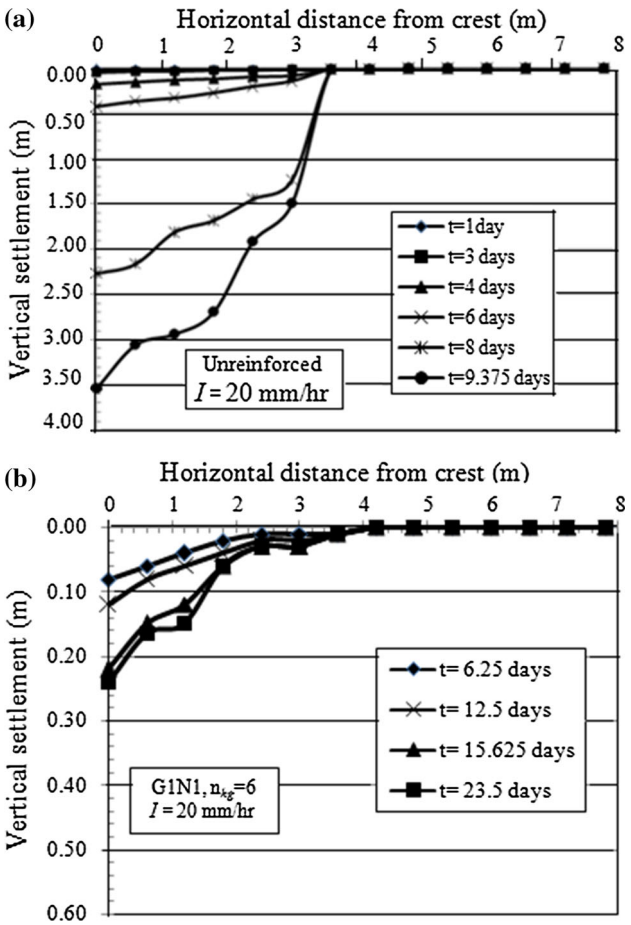

Fig. 5 Variation of surface settlements measured from crest of the slope with rainfall (in prototype dimensions). **a** Model T2, **b** Model T3

respect to a set of permanent markers shown in Fig. 2. Figure 6a, b present the deformation experienced by the model slopes, analyzed in terms of displacement vectors plotted on the original slope profile (in prototype dimensions), obtained by tracing the movements experienced by the plastic markers in horizontal and vertical direction for each selected image at fixed time intervals during rainfall. Figure 6a clearly depicts formation of a deep-seated global failure surface for the unreinforced slope model, along with considerable movement of the slope in horizontal and vertical directions. On the contrary, the model T3 reinforced with geocomposite (G1N1) in all six layers registered lesser movements with time in both horizontal and vertical direction, as evident from the position of displacement vectors plotted in Fig. 6b, thereby indicating the efficacy of dual-function geocomposite layers in maintaining slope stability under rainfall.

Figure 7a, b predict the displacements observed at the slope face with progress of rainfall, obtained by tracking the co-ordinates of inclined markers at the slope face in case of unreinforced slope (model T2), and that of plastic markers stuck to geocomposite layers facing towards the slope face for reinforced slope (model T3). The face movements have been plotted considering the slope face to be vertical, and coinciding with the vertical axis and origin at the toe. The corresponding $u/\gamma h$ values for PPT 4 placed at 350 mm distance (in model dimensions) from the toe of slope at different time intervals are indicated in Fig. 7a, b, which depicts an increasing trend with time, indicating slope movement with progress of rainfall. As evident from Fig. 7a, the unreinforced slope models T2 recorded a sudden displacement at the toe from an initial value of

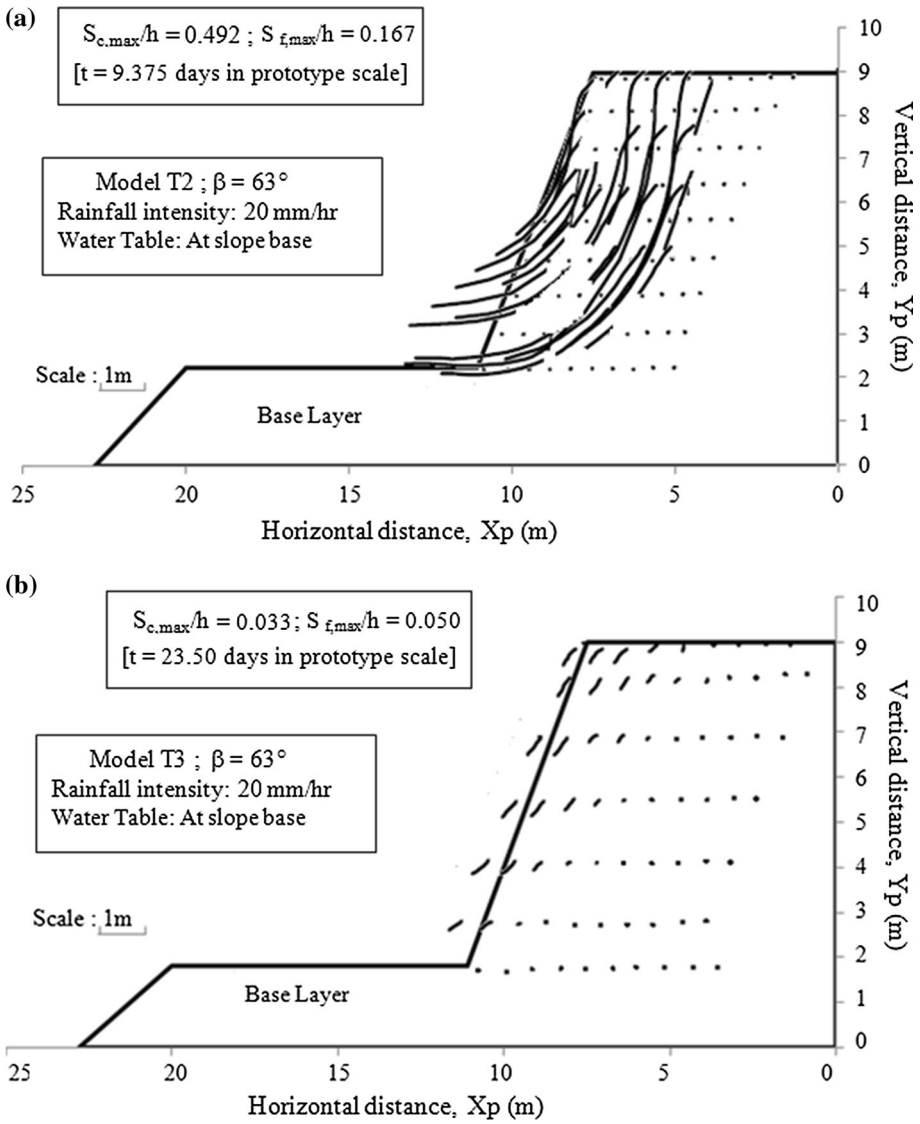

Fig. 6 Displacement vectors during rainfall obtained by image analysis. **a** Model T2 [unreinforced; rainfall intensity: 20 mm/h], **b** Model T3 [geocomposite reinforced; rainfall intensity: 20 mm/h]

0.15 m at t = 3.75 days to 1.20 m in prototype dimensions at the time of failure (t = 9.375 days). This may be attributed to the building up of pore water pressures within the slope due to rainfall, giving rise to positive seepage forces. On the contrary, the model slope T3 reinforced with geocomposite layers depicted negligible increase in lateral displacements of slope face with rainfall, the maximum value being 0.36 m in prototype scale (refer Fig. 7b).

Further, the strains experienced by the geocomposite layers with progress of rainfall were determined from the shift in coordinates of plastic markers glued onto the surface of the layers during preparation of model slopes (refer Fig. 3c). The maximum value of strain among the peak strains mobilized in individual reinforcement layers within the slope model was identified as the maximum peak strain value ($\varepsilon_{p,max}$), which is presented in Fig. 8 against normalized slope height (z/h). The model T3 reinforced with geocomposite layers (G1N1) exhibited low magnitudes of strain at all points of time with rainfall, the peak value ($\varepsilon_{p,max}$) being 8.01% at the termination of test (refer Fig. 8), which indicates slope stability against rainwater infiltration.

Conclusions

In the present paper, the potential of geocomposites (or hybrid geosynthetic layers) in improving the performance of low-permeable soil slopes subjected to rainwater infiltration was investigated by conducting centrifuge model tests on unreinforced and geocomposite reinforced slopes. The results indicated the efficacy of geocomposites in maintaining stability of slopes constructed with locally available (marginal) soils of low permeability. The above

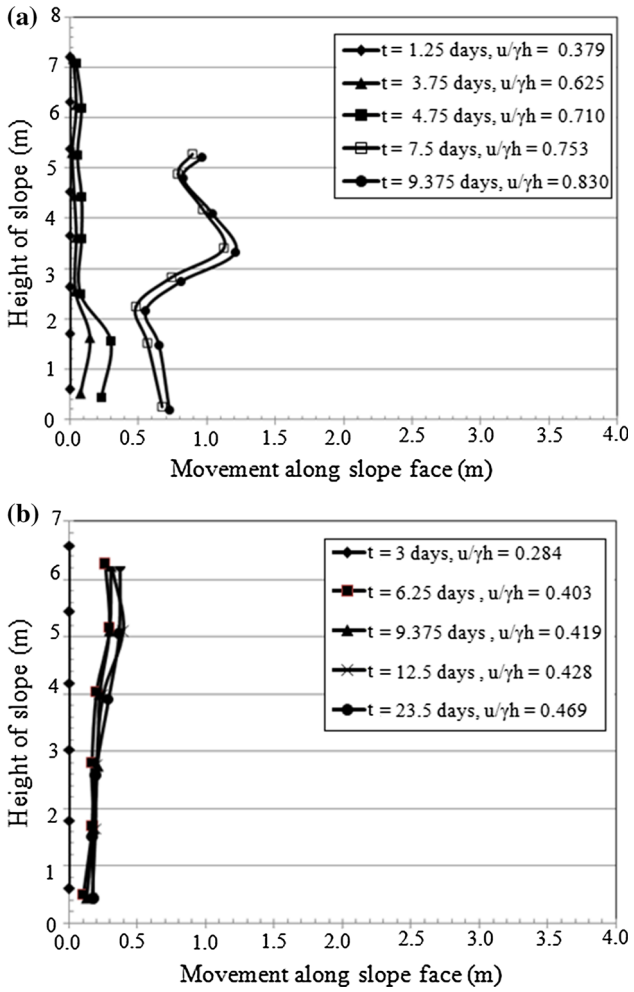

Fig. 7 Displacements at slope face during rainfall (in prototype scale). **a** Model T2 [Unreinforced], **b** Model T3 [Geocomposite reinforced]

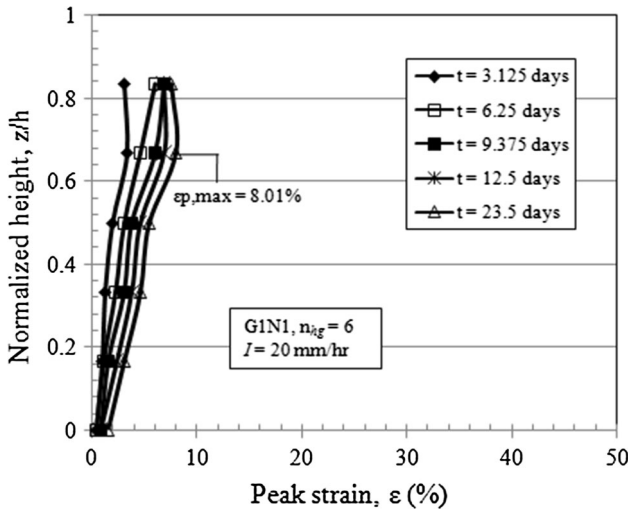

Fig. 8 Variation of peak reinforcement strain with rainfall [Model T3]

finding facilitates the use of soils available locally at the construction site in infrastructural projects, thereby preventing to a large extent the unsustainable over-mining of natural sand deposits for construction purposes. Further, based on analysis and interpretation of centrifuge test results, the following conclusions can be drawn:

1. The maximum settlement measured at the crest at failure increased by 24%, and positive pore water pressure levels due to rainfall rose by 17% in the model slope having an initial water table up to the base as compared to the slope model where ground water table was not simulated in-flight. This implies that, in the field, slopes having initial water table at relatively shallow depth have lower initial factor of safety, and are more susceptible to rainfall-induced failure as compared to the slopes having water table at a considerable depth below the base.
2. The inclusion of dual-function geocomposite layers within the slope resulted in reduction of excess pore water pressure values by about 47% on an average, indicating the importance of drainage function provided by geotextile component in maintaining slope stability under rainfall.
3. The surface settlements increased with rainfall for the unreinforced slope models due to gradual loss of soil matric suction and subsequent propagation of the wetting front, resulting in an eventual deep-seated global failure passing through the toe. On the contrary, the geocomposite reinforced slope model was stable for the entire duration of rainfall, and recorded negligible deformations with 93% lesser crest settlements as compared to the unreinforced low-permeable slope.
4. The maximum deformation at the slope face reduced by almost 70% with the incorporation of geocomposite layers, thereby indicating the efficacy of geogrid component in providing the necessary reinforcement function for maintaining slope stability under rainfall.
5. Further, the image analysis results indicated negligible movement of the geocomposite slope in both horizontal and vertical direction, and the maximum peak train ($\varepsilon_{p,max}$) recorded by the reinforcement layers was merely 8.01%. The above findings highlight the importance of coupling the functions of reinforcement and drainage simultaneously to maintain over-all stability of low-permeable soil slopes subjected to rainfall.
6. The present study focuses on the potential use of geocomposites (or hybrid geosynthetic layers) during construction of a new slope, where the geocomposite will be introduced as a flexible inclusion from the bottom to the top following the sequence of slope

construction. However, the above concept can be extended in case of existing steep slopes at or near their failure state by adopting permeable grout inclusions in association with stiffer anchors of high shear strength that can be 'nailed' into the slope (drainage anchors) to cater to the simultaneous requirements of reinforcement and drainage within the slope. However, this is beyond the scope of the present study and further investigations are warranted in this area.

Acknowledgements The authors would like to thank the members of National Geotechnical Centrifuge Facility at Indian Institute of Technology, Bombay for their support throughout the present study. In addition, the authors would like to thank the guest editors and reviewers for their constructive criticism in improving the quality of the manuscript.

References

1. CRED (Centre for Research on the Epidemiology of Disaster) (2012) Annual disaster statistical review 2011: the numbers and trends. CRED, Research Unit, Université Catholique de Louvain, Louvain-la-Neuve, Belgium
2. Dahal RK, Hasegawa S (2008) Representative rainfall thresholds for landslides in the Nepal Himalaya. Geomorphology 100(3–4):429–443
3. Basu D, Misra A, Puppala AJ (2015) Sustainability and geotechnical engineering: perspectives and review. Can Geotech J 52(1):96–113
4. Pathak YP, Alfaro MC (2010) Wetting-drying behavior of geogrid-reinforced clay under working load conditions. Geosynth Int 17(3):144–156
5. Koerner RM, Soong T-Y (2001) Geosynthetic reinforced segmental retaining walls. Geotext Geomembr 19(6):359–386
6. Yoo C, Jung HY (2006) Case history of geosynthetics reinforced segmental retaining wall failure. J Geotech Geoenviron Eng 132(12):1538–1548
7. Bhattacherjee D, Balakrishnan S, Viswanadham BVS (2012) Some studies on the seepage analysis of geosynthetic reinforced soil walls constructed with low-permeability backfill soil. In: Proceedings of the Indian geotechnical conference (IGC), Delhi, 13–15 Dec 2012, vol 1, pp 347–350
8. Bhattacherjee D, Viswanadham BVS (2014) Some studies on the performance of geocomposite reinforced slopes subjected to rainfall. In: Proceedings of the 8th international conference on physical modelling in geotechnics (ICPMG 2014), Australia, Gaudin & White (eds), Taylor & Francis Group (Pubs.), pp 1153–1159
9. Bhattacherjee D, Viswanadham BVS (2015) Numerical studies on the performance of hybrid-geosynthetic-reinforced soil slopes subjected to rainfall. Geosynth Int 22(6):411–427
10. Bhattacherjee D, Viswanadham BVS (2016) Effect of hybrid geosynthetic layers on soil walls with marginal backfill subjected to rainfall. In: Proceedings of geo-Chicago 2016, geotechnical special publication No 269, De A, Reddy KR, Yesiller N, Zekkos D, Farid A (eds), ASCE (Pubs.), pp 362–371
11. Viswanadham BVS, Bhattacherjee D (2015) Studies on the performance of geocomposite reinforced low-permeable slopes subjected to rainfall. Jpn Geotech Soc Spec Publ 2(69):2362–2367
12. Tatsuoka F, Yamauchi H (1986) A reinforcing method for steep clay slopes using non-woven geotextile. Geotext Geomembr 4(3–4):241–268
13. Mitchell JK, Zornberg JG (1995) Reinforced soil structures with poorly draining backfills. Part II: case histories and applications. Geosynth Int 2(1):265–307
14. Zornberg JG, Sitar N, Mitchell JK (1998) Performance of geosynthetic reinforced slopes at failure. J Geotech Geoenviron Eng 124(8):670–683
15. Iryo T, Rowe RK (2005) Hydraulic behaviour of soil geocomposite layers in slopes. Geosynth Int 12(3):145–155
16. Viswanadham BVS, König D (2004) Studies on scaling and instrumentation of a geogrid. Geotext Geomembr 22(5):307–328
17. Viswanadham BVS, Jessberger HL (2005) Centrifuge modeling of geosynthetic reinforced clay liners of landfills. J Geotech Geoenviron Eng 131(5):564–574
18. Rajesh S, Viswanadham BVS (2009) Evaluation of geogrid as a reinforcement layer in clay based engineered barriers. Appl Clay Sci 46(2):153–165
19. Raisinghani DV, Viswanadham BVS (2011) Centrifuge model study on low permeable slope reinforced by hybrid geosynthetics. Geotext Geomembr 29(6):567–580
20. Dell'Avanzi E, Zornberg JG, Cabral AR (2004) Suction profiles and scale factors for unsaturated flow under increased gravitational field. Soils Found 44(3):79–89
21. Tamate S, Suemasa N, Katada T (2010) Simulating shallow failure in slopes due to heavy precipitation. In: Proceedings of the 7th international conference in physical modelling in geotechnics—7th ICPMG, Switzerland, Springman S, Laue J, Seward L (eds), Taylor & Francis group (Pubs.), vol 2, pp 1143–1149
22. Bhattacherjee D, Viswanadham BVS (2017) Design and performance of an inflight rainfall simulator in a geotechnical centrifuge. Manuscript accepted in Geotechnical Testing Journal, ASTM, Paper-ID: GTJ-2016-0254.R1
23. Chandrasekaran VS (2001) Numerical and centrifuge modelling in soil structure interaction. Indian Geotech J 31(1):30–59
24. Image-Pro Plus (2004) Image-Pro Plus Manual. Version 5.1. Media Cybernetics, Inc., USA